ISPRS Journal of Photogrammetry and Remote Sensing ▮ (▮▮▮▮) ▮▮▮–▮▮▮

Contents lists available at ScienceDirect

ISPRS Journal of Photogrammetry and Remote Sensing

journal homepage: www.elsevier.com/locate/isprsjprs

Real-time registration of airborne laser data with sub-decimeter accuracy

Jan Skaloud *, Philipp Schaer, Yannick Stebler, Phillip Tomé

TOPO Lab, École Polytechnique Fédérale de Lausanne, Station 18, 1015 Lausanne, Switzerland

ARTICLE INFO

Article history:
Received 17 July 2009
Received in revised form
21 December 2009
Accepted 27 December 2009
Available online xxxx

Keywords:
LIDAR
Georeferencing
GPS/INS
Real-time-laser scanning
Accuracy

ABSTRACT

This paper presents a methodology for the precise registering of airborne laser data directly in flight with an accuracy that is sufficient for the majority of derived products, such as digital terrain models. We first present the strategy that integrates GPS/INS/LiDAR data for generating laser point clouds directly in flight and analyzes their accuracy. The latter requires the implementation of a functional covariance propagation on-line for all the system components (i.e. trajectory, laser, system calibration) to which influences of scanning geometry are added at the end of a flight line. The study of scanning geometry necessitates the classification of vegetation and coarse estimation of the terrain normal. This is achieved by a method that we formerly proposed for off-line quality analysis. The second part of the paper focuses on the positioning component. In high resolution scanning performed close to the terrain, the absolute accuracy of the resulting point cloud depends mainly on the quality of the trajectory which is related to the type of GPS solution (e.g. absolute positioning, DGPS, RTK). To reach sub-decimeter accuracy for the point cloud in the real-time, an RTK-GPS solution is needed. This requires the establishment of a communication link for the transmission of GPS corrections (or measurements). We analyze the usability of RTK-GPS/ALS acquired during several flights using different communication methods in the particular context of helicopter based missions. We focus mainly on the exploitation of nation-wide reference GNSS networks and confirm experimentally that the real-time registration of airborne laser data is feasible with sub-decimeter accuracy. Such quality is sufficient not only for a wide range of applications, but it also opens new opportunities for monitoring missions that require a short reaction time. Finally, we concentrate on situations when the phase and code corrections cannot be transmitted, and the quality of the differential carrier-phase positioning needs to be predicted. We validate the previously introduced indicators of positioning quality by simulated degradation of the input data.

1. Introduction

Airborne Laser Scanning (ALS) is a very effective and accurate method for establishing detailed terrain models from airborne platforms. In some applications the requirements on point density and DTM accuracy can be as high as several points per m^2 and 0.1 m, respectively. The factors affecting laser-target position accuracy are numerous (Schenk, 2001). Nevertheless, the detailed analysis of error contributions (Glennie, 2007) shows that in close and mid-range airborne missions more than half of the ALS error budget is attributed to the positioning (Fig. 1). Hence, high quality positioning becomes a crucial factor for a laser scanning mission of such a type.

1.1. Conventional approach to ALS

Contrary to the terrestrial laser scanning (TLS), the conventional airborne laser scanning generates the point-cloud coordinates only after the mission. There, the laser data is merged with the trajectory in a process that is sometimes referred to as 'basic-processing'. For mapping tasks of higher accuracy, the trajectory estimate requires integrating inertial and satellite observations from the rover and one or more base receivers. The base-receiver data is normally made available only after the flight and therefore the integrity of the carrier-phase differential positioning (CP-DGPS) can be obtained only then. If the quality of CP-DGPS is insufficient for periods longer than 10 to 30 s, there is a high probability that the quality of the GPS/INS integrated trajectory will also be insufficient during this interval. In some cases, the resulting positioning error has a constant influence during the flight-line. Then, its effect could be mitigated by the strip adjustment supposing there is a good overlap between the adjunct strips, e.g. Filin and Vosselman (2004) and Pfeifer et al. (2005). In most cases, however, there is some dynamic fluctuation in the phase data observations, or in the satellite constellation, the reasons for which the assumption of constant trajectory errors are not valid (Skaloud, 2006). The same is true in corridor-mapping, where the internal point-cloud accuracy cannot be judged from inter-strip discrepancies. In such scenarios, the

* Corresponding author. Tel.: +41 21 693 2753; fax: +41 21 693 5740.
E-mail address: jan.skaloud@epfl.ch (J. Skaloud).

0924-2716/$ – see front matter © 2010 International Society for Photogrammetry and Remote Sensing, Inc. (ISPRS). Published by Elsevier B.V. All rights reserved.
doi:10.1016/j.isprsjprs.2009.12.003

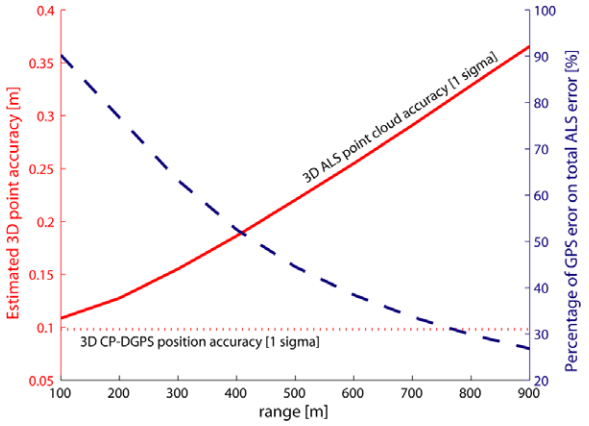

Fig. 1. Estimated contribution of the carrier-phase differential GPS position error to the overall point-cloud accuracy for a representative ALS system defined as: Optech's ALTM3100 with Applanix 310 inertial navigation unit and corresponding calibration accuracies.

remaining alternative for improving data quality is re-flying the mission, or at least part of it. This alternative is not only costly, but maybe also not feasible under some circumstances (e.g. monitoring applications that support decision making, short-data delivery, etc).

1.2. RTK approach to ALS

As mentioned in Skaloud (2006) there are a number of possibilities for checking the quality of the satellite measurements in flight, most of them coming from avionics (Ober, 2001). Nevertheless, as the demand on trajectory accuracy in ALS applications is usually higher, the approaches pursued in avionics can only be regarded as complementary. The best control for checking the quality of the phase observations is performing CP-DGPS positioning in real-time. In the surveying community, this approach is called Real-Time-Kinematics (RTK) and requires establishing and maintaining communication between the rover and the base receivers. This concept is certainly challenging for airborne rovers when relying on publicly available methods of mobile communication that are restrained as regards coverage (e.g. radio power or mobile-phone infrastructure) or continuity (i.e. dynamic allocation of service in radio-packed transmission as GPRS). This paper aims to demonstrate that, although demanding in realization, the RTK approach is feasible for helicopter-based ALS missions, at least in a European-like communication infrastructure. In situations where such a solution is not possible we propose an alternative indicator that predicts the quality of the differential positioning, including the carrier-phase data solution.

1.3. Paper outline

To take the full benefit of the RTK positioning, the whole chain of basic processing needs to be implemented on-line. Such implementations generally do not exist in commercial systems; therefore, we first explain the conceptual configuration that offers such a possibility. Then we recall the definition of ALS system errors and the developed functional model for their on-line recovery. Besides the normally considered error sources, we present the integration of the time-delayed estimation of the scanning geometry (Schaer et al., 2007) into the strip-wise quality map. The next part of the paper presents a real-time GPS quality monitoring tool, and modern methods for achieving an in-flight RTK solution. These approaches are then tested in real operations and the results are presented. The subsequent discussion concentrates first on analyzing the registration accuracy of the trajectory and the point cloud with respect to the post-processing. Finally, we focus on the (general) case where no RTK is possible due to the absence of the communication link and we analyze the predicted quality attribute under a simulation scenario. The conclusions are drawn after that.

2. Real-time registration methodology

2.1. General architecture

The registration of the ground coordinates $\mathbf{x}_p^e(t)$ of a laser return p at time t in Earth-Fixed-Earth-Centered frame (e) is calculated by combining the information from the scanner, the GPS/INS measurements and calibration parameters as:

$$\mathbf{x}_p^e(t) = \mathbf{x}_b^e(t) + \mathbf{R}_l^e(\varphi(t), \lambda(t))\,\mathbf{R}_b^l(r(t), p(t), y(t)) \times \mathbf{R}_s^b(\omega, \varphi, \kappa)\left(\mathbf{x}_b^s + \rho(t)\begin{bmatrix}0 & \sin\theta(t) & \cos\theta(t)\end{bmatrix}^T\right). \quad (1)$$

Thereby,

$\mathbf{x}_b^e(t)$ is the position of the navigation/body frame (b) center expressed in the e-frame at the same time,

$\mathbf{R}_l^e(\varphi(t), \lambda(t))$ is the orientation of the local-level frame (l) at latitude $\varphi(t)$and longitude $\lambda(t)$with respect to the e-frame,

$\mathbf{R}_b^l(r(t), p(t), y(t))$ is the GPS/INS estimated orientation of the b-frame with respect to the local-level frame parameterized by three Euler angles, roll, pitch and yaw.

$\mathbf{R}_s^b(\omega, \varphi, \kappa)$ is the relative orientation between the b-frame and the laser scanner frame (s) due to the mounting (the calibrated part of this matrix is also referred to as boresight) parameterized by three Euler angles, omega, phi and kappa.

$\mathbf{x}_b^s$ is the spatial offset (also referred to as the lever-arm) between the b-frame and the s-frame origins,

$\rho(t), \theta(t)$ are the LiDAR range and encoder-angle measurements, respectively.

The on-line registration of airborne LiDAR data according to Eq. (1) is practically nonexistent in commercial ALS. This section briefly presents a custom-made system which has the benefit, among others, of such functionality. We have built up this system upon its commercialized predecessor and we call it Scan2map (Schaer et al., 2008). It integrates multiple-frequency GNSS receivers with a tactical-grade inertial measurement unit (IMU), a mid-range airborne laser scanner and a medium format digital camera. The system is mainly adapted for helicopter-based surveys, with the sensor head suspended on its side. The integration of all data streams is performed in a modular architecture with an Ethernet linkup. We claim that the adopted integration approach is portable to other systems provided that the basic acquisition modules are adapted for re-transmitting the necessary information according to a predefined interface.

As shown in Fig. 2, the data acquisition components are followed by two integrating modules: the module for real-time GPS/INS integration named GIINAV and the module for LiDAR exterior orientation called LIEOS. The supervisory and flight-management role is accomplished by a module named HELIPOS. Within a flight-line, the LIEOS module focuses on processing all LiDAR measurements and on generating a laser point cloud in real-time. Once the strip is terminated, its quality gets analyzed within the software sub-module named LIAN. There, the data can be also classified, and a coarse digital surface/terrain model can be produced (Schaer et al., 2008). The precision of the obtained laser point cloud is directly related to the precision of the trajectory. Therefore we first recall the presentation of the trajectory and the LiDAR registration modules, respectively, before concentrating on the real-time accuracy estimation.

2.2. Real-time trajectory estimation

The navigation module GIINAV is the real-time strapdown inertial navigator and GPS/INS data integrator. The integration is

Please cite this article in press as: Skaloud, J., et al., Real-time registration of airborne laser data with sub-decimeter accuracy. ISPRS Journal of Photogrammetry and Remote Sensing (2010), doi:10.1016/j.isprsjprs.2009.12.003

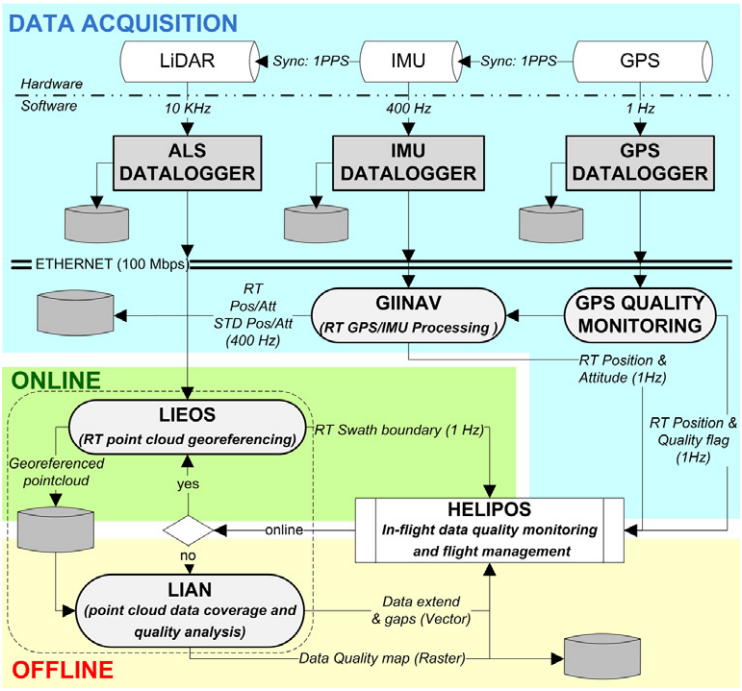

Fig. 2. Overview of the multi-modal architecture adapted for ALS on-line registration and quality assessment.

performed via a loosely-coupled Extended Kalman Filter (EKF) with a 22 error-state vector (Tome et al., 2000). The inertial data are processed in its original sampling (i.e. 400 Hz in the actual configuration of the Scan2map), while the GPS data rate is typically set to one second. The critical part of the integration algorithm is concerned with the initialization of orientation, a non-trivial issue especially for the helicopter-born flights. For that reason, the operator has the option to perform either transfer, static or dynamic alignment. For maximum operational flexibility the static initialization can be constrained to a very short time if the approximate heading is specified using external information (i.e. magnetic reading). Nevertheless, the implemented model uses a customized version of the large-heading error model (Kong et al., 1999) and tolerates well large initial uncertainties. Hence it is possible to completely initialize or re-initialize the system in flight without imposing much restriction on the dynamics (even for a helicopter). The precision of the positioning is closely related to the GPS-positioning mode, which will be discussed later.

2.3. Real-time point cloud generation

The role of the georeferencing module is twofold: First, to generate the laser point cloud while on a flight-line, then, to analyze its quality. The first task is a real-time operation handled by the LIEOS module, while the other is a delayed process handled by the LIAN (LiDAR ANalyse) element. LIAN is not a stand-alone application but a separate thread of lower priorities that is entirely managed by LIEOS. Its functionality with respect to monitoring the scanning coverage (extent) and point density was presented in Schaer et al. (2008). Its new capability for accuracy tracking will be described separately in the following section. As shown in Fig. 2. the inputs to LIEOS are the LiDAR line data and the real-time trajectory estimate at adaptable data rates. The system operator toggles between two operating modes of this program. At the beginning of a flight line the operator presses the 'on-line' button so that LIEOS computes and stores all laser point-cloud coordinates into a file and transmits points related to swath characteristics (i.e. boarders and nadir) to the flight-management program for displaying. At the end of a flight line the operator toggles the system 'off-line', which stops point-cloud calculation and the transmission of swath boarders. At the same time, the data analysis tool (LIAN) is started as a separate thread to evaluate the scanning coverage (extent), point density and data quality. The data extent information is sent to the flight-management tool (HELIPOS) in the form of vector boundaries, while the point density information is displayed in the same environment as a raster image. Similarly, the data *quality* factors that will be described later are also presented as a raster image and the operator can access them when the LIAN thread finishes analyzing the data. One of the reasons for separating the two main tasks in time (i.e. the real-time data registration vs. data analysis) is to keep the CPU requirements at a reasonable level. Performing both tasks in parallel would significantly reduce the computational speed and threaten the real-time monitoring capacity. Moreover, this approach guarantees that the more computationally demanding analyses (such as the error propagation) are carried out only over the areas of interest and at a predefined sampling rate.

The LIEOS module supports different projections and datums, the choice of which is usually influenced by the datum and projection on the map used for the guidance. The georeferencing algorithms implemented in the LIEOS were optimized to allow processing throughput of 'tens of thousands' of points per second considering that the computational load per laser-return is influenced by several factors such as: the frequency of trajectory output, the selected coordinate system and choice of the georeferencing/registration algorithm. These factors may vary per system or its setup (e.g., the scanner repetition rates may vary from 30 to 180 kHz, trajectory sampling from 0.01 to 2 kHz), while the availability of processing power depends on the distribution of individual applications and the processor speed. In our case the trajectory output at 400 Hz is further interpolated to the 30 kHz pulse repetition rate of the scanner. Nevertheless, to allow general applications, three georeferencing methods were implemented and their choice is left to the user:

- The 'fast option' is an approximate method of sub-meter accuracy that is especially advantageous if the point cloud is requested in geographical coordinates.

Please cite this article in press as: Skaloud, J., et al., Real-time registration of airborne laser data with sub-decimeter accuracy. ISPRS Journal of Photogrammetry and Remote Sensing (2010), doi:10.1016/j.isprsjprs.2009.12.003

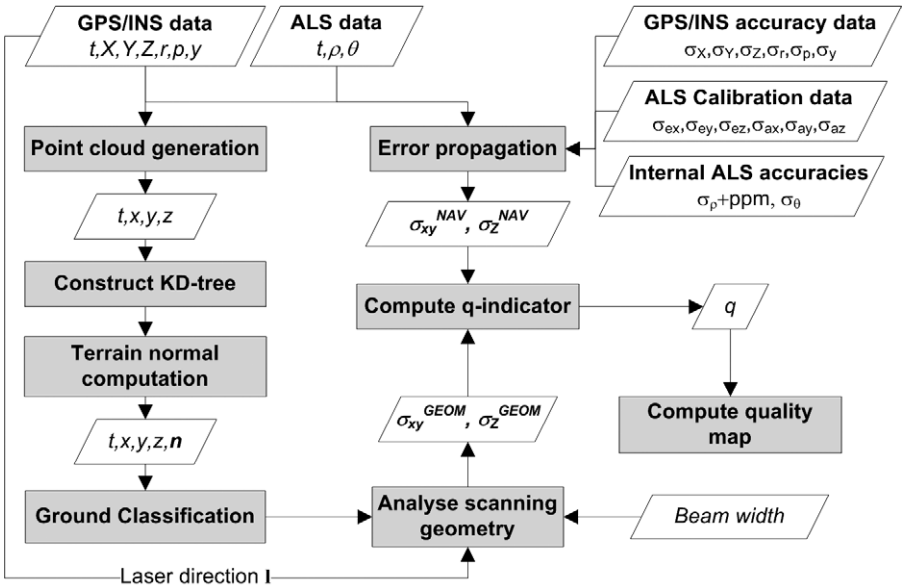

Fig. 3. Workflow for point-cloud quality assessment and quality map computation.

- The 'approximate method', which despite its name provides residual distortions at sub-centimetre level (in most flight scenarios) and regardless of the terrain characteristics (Legat, 2006). Its choice is especially advantageous if (a) the point registration is requested in the national coordinates, (b) the ratio scanner versus trajectory sampling is relatively high.
- The 'rigorous method' that is optimized for speed, but uses no approximations. It performs the calculation of the laser point-cloud coordinates in a Cartesian system and then applies its rigorous transformation to the specified datum and projection. Although this method is more computationally demanding, its application within the presented system (10 kHz laser sampling) requires no more than 10%–15% of the total computing capacity of the on-board processor.

2.4. Accuracy monitoring

The approach for the accuracy monitoring is schematically shown in Fig. 3. In the first place the random errors are propagated through the functional model of the laser data registration equation (Eq. (1)). This yields a 3×3 covariance matrix for each laser return:

$$\mathbf{C}_{xyz} = \begin{bmatrix} \sigma_x^2 & \sigma_{xy} & \sigma_{xz} \\ \sigma_{xy} & \sigma_y^2 & \sigma_{yz} \\ \sigma_{xz} & \sigma_{yz} & \sigma_z^2 \end{bmatrix} = \mathbf{F} C_{ll} \mathbf{F}^T. \quad (2)$$

The functional model (matrix $\mathbf{F}$ in Eq. (2)) is obtained by the Taylor expansion of Eq. (1) and by truncating the resulting series after the first term. To speed up the computations, we have constructed the functional model by algebraic derivation. Thereby, $\mathbf{F}$ takes the form of:

$$\mathbf{F}_{3\times 14} = \left[\mathbf{F}_{pos} | \mathbf{F}_{att} | \mathbf{F}_{leverarm} | \mathbf{F}_{bore} | \mathbf{F}_{range} | \mathbf{F}_{encoder}\right]. \quad (3)$$

With the simplifying assumption that all individual error sources are uncorrelated, the stochastic model is given as

$$\mathbf{C}_{ll_{14\times 14}} = \mathrm{diag}\left(\left[\sigma_{x_b^e}^2 \quad \sigma_{y_b^e}^2 \quad \sigma_{z_b^e}^2 | \sigma_{roll}^2 \quad \sigma_{pitch}^2 \quad \sigma_{yaw}^2 | \right.\right.$$
$$\left.\left. \sigma_{x_b^s}^2 \quad \sigma_{y_b^s}^2 \quad \sigma_{z_b^s}^2 | \sigma_\omega^2 \quad \sigma_\varphi^2 \quad \sigma_\kappa^2 | \sigma_\rho^2 | \sigma_\theta^2 \right]\right) \quad (4)$$

where the elements related to the trajectory are dynamically estimated by the Kalman Filter used for GPS/INS data integration. Those related to the system placement (i.e., lever-arm and boresight) are determined from the calibration and can be considered constant in time (Skaloud and Lichti, 2006).

The accuracy parameters related to the scanner (range, encoder) in Eq. (4) are provided by the manufacturer for an orthogonally oriented target and nominal distance. The range variance is therefore adapted in time according to the observed distance. The impact of the incident angle is added later once we obtain information on the scanning geometry that requires a knowledge of the terrain normal (Schaer et al., 2007). The terrain normals are computed at the end of a flight line using the local covariance method (Bae and Lichti, 2004). Such a method of estimation is only reliable when the neighbourhood of the laser points forms approximately a planar surface. For example, laser points on vegetation have no clear geometric structure; hence the derived normal is geometrically not interpretable. As a consequence, such points need to be removed. This is performed by means of an automated ground classification algorithm that we proposed in Schaer et al. (2007). We implemented a computationally optimized version of the same algorithm, the execution of which starts in the background (as a separate thread) once a flight line gets completed. The additional variances reflecting the influence of the scanning geometry are decomposed into horizontal and vertical elements, i.e., $\sigma_{xy}^{2_{geom}}$, $\sigma_z^{2_{geom}}$ respectively (Eq. (5)).

Once all components contributing to the ALS error budget are assessed, they are regrouped into one unique quality attribute. This quality indicator q for a laser point i is constructed as an accumulation of random errors coming from the error propagation of the laser registration equation (Eq. (2)) and the scanning geometry analysis:

$$q_i = \sqrt{\mathrm{trace}\left(\mathbf{C}_{xyz_i}\right) + \sigma^{2^{geom}}_{xy_i} + \sigma^{2^{geom}}_{z_i}}. \quad (5)$$

As previously explained, these so-called q-factors are calculated for every point, but their representation is regrouped into a raster image of a predefined resolution (Fig. 4). The operator can view this image once the analysis of data quality is completed by the LIAN thread.

3. Trajectory solutions

As previously mentioned, the trajectory estimator uses a loosely coupled GPS/INS data integration. With the employment of a

Please cite this article in press as: Skaloud, J., et al., Real-time registration of airborne laser data with sub-decimeter accuracy. ISPRS Journal of Photogrammetry and Remote Sensing (2010), doi:10.1016/j.isprsjprs.2009.12.003

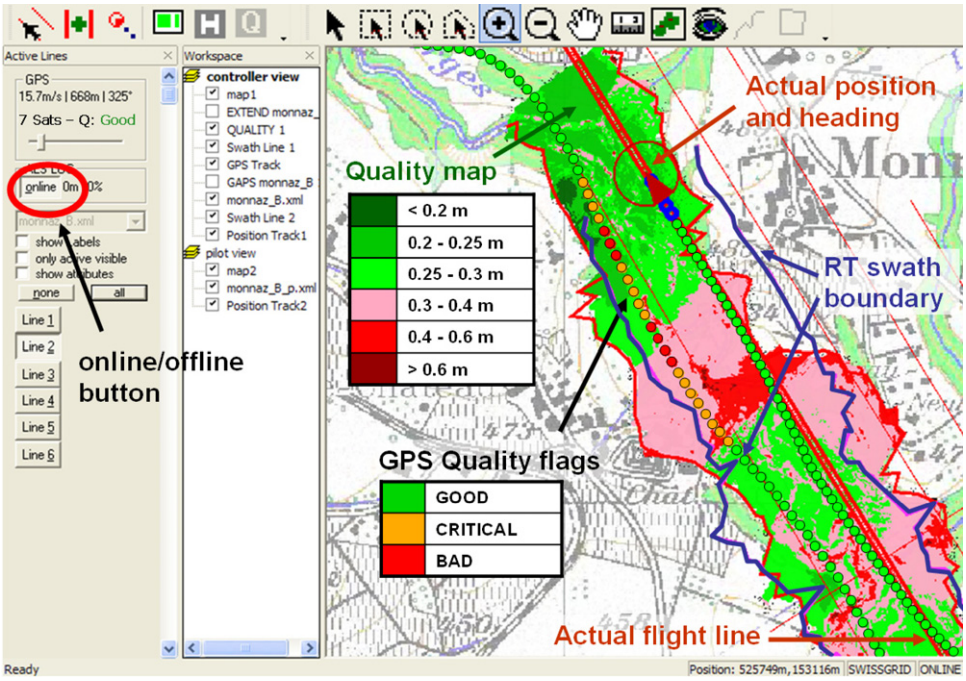

Fig. 4. Example of displaying real-time quality data (swath, GPS quality flag, q-indicator).

tactical-grade IMU (i.e. mid-range precision), the uppermost importance for the accuracy of the final point cloud lies on the GPS data quality. Therefore, the in-flight GPS quality assessment represents a crucial step in the whole processing chain. Poor positioning quality can originate from different problems, spanning from poor satellite constellation (resulting in too few satellites or less favourable geometry), cycle slips in the phase observations, to a poor signal-to-noise ratio (i.e. interferences, jamming, etc.). When monitoring the positioning performance, we distinguish two cases according to the availability of the communication link (i.e. RTK possible or not). The following describes a more general case.

3.1. Point positioning with differential phase-quality prediction

The proposed monitoring tool disposes of a set of indicators (see Fig. 5) used for quality evaluation:

1. Solution type: if the communication line between the rover and a reference station gets established and RTK is enabled, the ambiguities can be solved "on-the-fly", yielding the best possible estimate for achievable CP-DGPS quality. This option together with the accuracy estimate represents the 'ultimate control' of the phase-data quality and will be described in the following section.
2. Analysis of the GPS constellation (DOP values, number of visible satellites, etc.).
3. L1/L2 carrier phase tracking loop monitoring: In general, L2 is more affected by signal degradation than L1 due to lower transmitting power. Therefore, monitoring the availability of the L2 signal is important for detecting quality degradations.
4. RAIM (Receiver Autonomous Integrity Monitoring): Nowadays most high quality GPS receivers used in kinematic applications are RAIM equipped. The RAIM enables analyzing the GPS integrity and consistency on the basis of code measurements only. More details about RAIM can be found in Van Diggelen and Brown (1994).
5. Cycle slip detection on L1: Using the velocity trend method proposed in Xu (2007), the ambiguity time difference $\Delta_t N_i = N_i(t) - N_i(t-1)$ for satellite i can be computed as the temporal difference between the phase $\Delta_t \Phi_i$ and integrated Doppler observations D_i:

$$\Delta_t N_i = \Delta_t \Phi_i - \int_{t-1}^{t} D_i \mathrm{d}t + \varepsilon. \tag{6}$$

Finally, the status of the individual indicators is combined into one final quality flag that can be immediately presented to the system operator (see Figs. 4 and 9). The quality flag has three levels:

I. Good: The ambiguities can be fixed in post-processing. The expected 3D position accuracy should be below 0.1 m.
II. Critical: The ambiguities are likely to be resolved only partially or with low reliability. The GPS position accuracy is expected to be between 0.1 and 0.5 m.
III. Bad: The ambiguity fix is not possible, the expected accuracy equals to the float ambiguities or to carrier-smoothed code solution (expected positioning accuracy > 0.5 m).

Using these flags, the covariance of the GPS point positioning (used as input into the real-time GPS/INS integration) can be adapted accordingly. This yields more realistic position accuracy estimates (obtained from the real-time GPS/INS integration) which are subsequently used as input values for the real-time error propagation.

3.2. RTK

Communication link(s) are required for the real-time transmission of the GPS measurements or its corrections from the base station(s). The transmission possibilities of this information range from (geostationary) satellites to terrestrial wireless data transmission techniques. The satellite based concept is usually limited to code-corrections (e.g., SBAS), the accuracy of which is not sufficient, or is slow in convergence (e.g., OmniSTAR). The reasons related to bandwidth, interference, coverage or cost further limit the relatively wide range of possibilities to two sources for performing RTK: radio and cell-phone related technologies.

The transmission by radio is used in the traditional RTK applications (i.e. surveying). Its inconvenience for ALS is the limited

Please cite this article in press as: Skaloud, J., et al., Real-time registration of airborne laser data with sub-decimeter accuracy. ISPRS Journal of Photogrammetry and Remote Sensing (2010), doi:10.1016/j.isprsjprs.2009.12.003

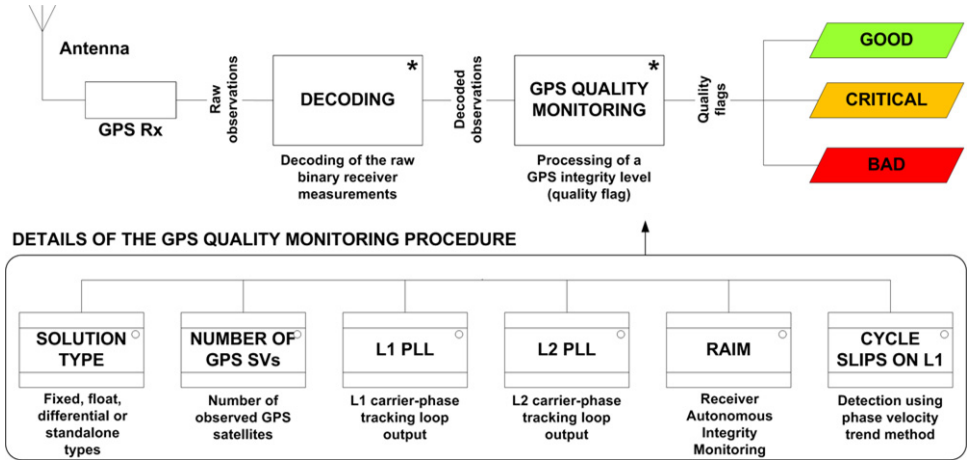

Fig. 5. Overview of real-time GPS quality monitoring tool.

range that is related to the (relatively low) transmission power. As the weight (essentially of power supply) is not critical here, the range can be extended using either ground repeaters or increased transmission power as long as the legal requirements are respected.

The second generation of the Global System for Mobile communications (GSM) is limited by its data rate of only 9.6 kbps. That corresponds approximately to 5 Hz of dual-frequency measurements from one reference station. The problems related to cell registration and the hand-over between the cells are known to occur for fast moving carriers, such as aircraft. On the other hand, the General Packet Radio Service (GPRS) that is available on practically all GSM networks does not suffer such setbacks and has four times more bandwidth (i.e. four voice channels). The more recent UMTS technology can handle even higher data transfer rates; however, the transmission is usually handled by 'bursts' of packets, and the communication has varying latency. Hence, this approach is less suitable for RTK positioning than GPRS. Although the cell-network coverage decreases in rural regions, the coverage in European countries is good and constantly spreading. Accessing data correction via GPRS is simple (i.e. service use is directly added to the communication charges) in many European states equipped with permanent GNSS networks. The type of the service may vary according to the implemented technology; however, most networks adopt the instant Virtual Reference Station (VRS) approach. In this case the broadcasted corrections are interpolated from three permanent stations that are closest to the requested position of a 'virtual' base. That was also the case in the tested flights conducted in Switzerland.

4. Analysis of registration

The described approach of precise real-time ALS with in-flight accuracy analysis has been tested on several flights in 2009 where the Scan2map system was carried by a helicopter. In this section we provide the synthesis of our experience with respect to the RTK trajectory accuracy and the achieved accuracy of the real-time generated point cloud. Considering that the results are comparable among the flights based on GSM/GPRS communication and nationwide VRS, we have chosen one flight of such type. Its performance will be evaluated in comparison with another flight using a real base station and radio link.

The positioning conditions were favorable for both data sets, with good satellite geometry and in the case of radio, close separation from the reference receiver. The flight lines were relatively short (a few minutes) and high-dynamic turns were executed between them. The rapid change in direction and the increased horizontal acceleration make the systematic errors within the inertial system well observable through GPS position and velocity updates, while flight lines of short duration limit their accumulation. These facts, together with the low-flying height, contributed to the good determination of the referenced GPS/INS trajectory obtained by post-processing ($1\,\sigma$ position per coordinate < 5 cm, $1\,\sigma$ orientation $< 0.01°$).

4.1. RTK- trajectory accuracy

The two upper plots in Fig. 6 show an extract of the difference in trajectory estimation expressed in a local frame between the real-time solution (using RTK-GPS and GIINAV real-time GPS/INS integration) and the post-processed results for the GPRS/VRS flight. As differences in the East and North components are similar, only the latter is shown here. The upper horizontal bars indicate periods when the system was on a flight line (and thus the results are of higher importance). The obtained differences for fixed RTK positions are mostly below 0.1 m in altimetry and planimetry, respectively. Nevertheless, the effects of float (horizontal bar areas) and standalone (vertical lines in the North and Height plots) solutions are demonstrated through sudden accuracy losses. They occur mainly during the transition phases of the flight when the GNSS signal reception is affected either by obstructions due to the environment (high mountains) or by the communication hand-over between GSM cells (an effect observable in high-speed trains). It should be noticed that even in the post-processing step the ambiguities could not be resolved for a portion of the flight. This fact highlights the importance of monitoring the RTK ambiguity status within the flight as it identifies the potential problems in the carrier-phase post-processing step.

The two lower plots of Fig. 6 depict an extract of the differences in attitude. Since the roll and pitch differences are very similar, only the former ones are represented here. These differences were expected for forward filtering with this type of IMU (Litton LN-200). For both cases, the roll/pitch Root Mean Square (RMS) value is below 0.05°. The yaw RMS is naturally higher because of its dependence on the flight dynamics and alignment accuracy, but it remains below 0.10°.

In the RTK-radio/fixed-base flight, the positioning differences between PP-RTK within the flight-lines were also kept at 0.1 m (RMS) with maximum errors at 0.2 m in planimetry and 0.4 m in altimetry. The attitude accuracy was identical to that described previously (Fig. 6). The monitoring of the radio signal quality revealed that the reception of the data tends to fade away during the transfer period of the flight and in the turns where the receiver antenna is no longer oriented vertically. On the contrary, the

Please cite this article in press as: Skaloud, J., et al., Real-time registration of airborne laser data with sub-decimeter accuracy. ISPRS Journal of Photogrammetry and Remote Sensing (2010), doi:10.1016/j.isprsjprs.2009.12.003

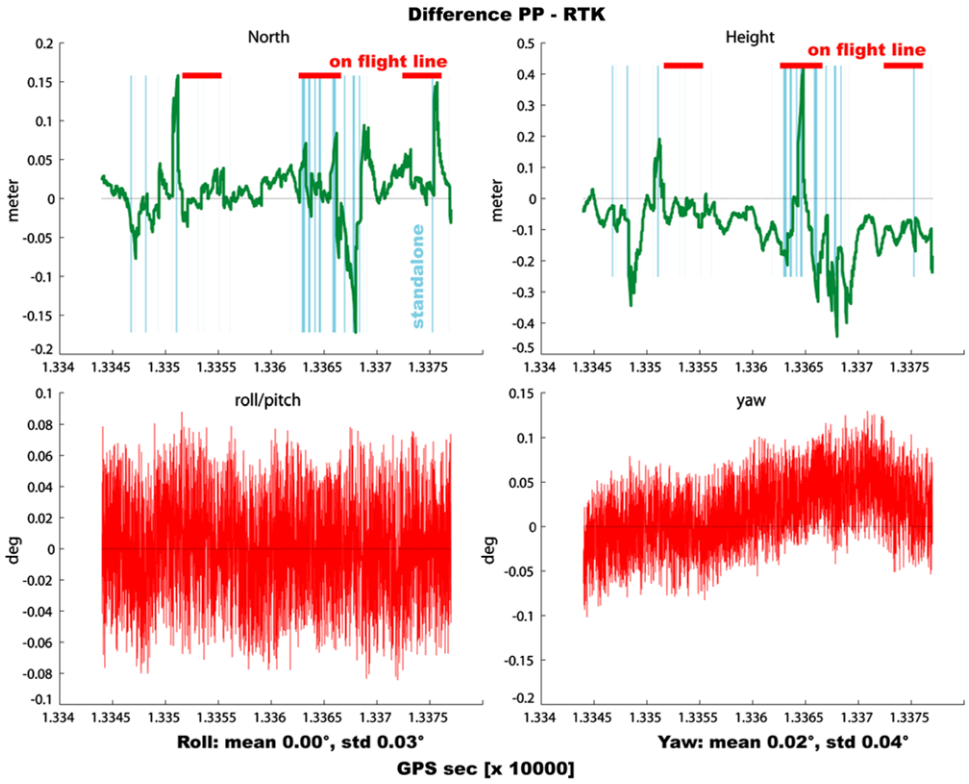

Fig. 6. Difference in the computed position and attitude between the real-time solution using RTK-GPS (RTK by radio) and post-processed solution using CP-DGPS.

GPRS communication link was always available in other flights using this technology. There, the losses of fixed ambiguities were mainly caused by GPS signal obstructions. This problem was also noticeable during the carrier-phase post-processing step.

4.2. RTK-generated point cloud

The Tables 1 and 2 summarize differences in the post-processed versus the real-time estimates of the laser point cloud for both flights. They also show the percentage of observations obtained in each type of GPS solution as well as the mean differences and standard deviation along the three axes. The *XYZ* column presents RMS of 3D vector magnitude. It can be seen that the proportion of fixed and float solutions is higher in the GPRS/VRS configuration, highlighting the good availability of the GPRS network in the flown region. Although the data lengths are different, the proportional distribution of the RTK-fixed solutions and the 3D discrepancies remain similar for both flights.

The histograms in Fig. 7 show distribution of the laser point-cloud coordinate differences (post-processed minus RTK-ALS solution) obtained in the flight using corrections over GPRS. It can be shown by the forward covariance propagation that the position errors directly influence the accuracy of the georeferenced point cloud, (e.g. Glennie, 2007). According to that, the point coordinate errors along the three axes are similar to the GPS errors depicted in Fig. 6: the planimetric and altimetric accuracies remain within a range of 0.1 m (Table 2). It can be deduced that the GPS data outages of shorter duration or the isolated float and standalone positioning solutions are successfully surmounted through adequate stochastic modelling in the real-time GPS/INS integration. For other flights these distributions are very similar or better (3D RMS < 0.05 m) and therefore not shown here. In our best experience, the RTK positioning with fixed ambiguities was maintained throughout all flight lines and differed from the post-processed results only at the cm-level.

5. Analysis of quality indicators

In the previous section we evaluated the quality of the real-time generated point cloud. We now concentrate on validating the predicted confidence levels for its estimation. The covariance propagation presented in Section 2 was previously validated in calibration (Skaloud and Lichti, 2006) as well as in separate investigations related to scanning geometry (Schaer et al., 2007). For this reason we pay more attention to critical component of the positioning. As explained before, such a prediction is especially useful in cases where the phase and code corrections cannot be (or are not) transmitted, and the post-processed quality of the differential carrier-phase positioning and that of the point cloud need to be predicted. In the following we will confirm the pertinence of the formerly introduced positioning quality indicators through a simulated scenario that uses degradation of the input data.

5.1. Approach

Accessing the absolute accuracies of the individual laser returns is a laborious and challenging task due to the high amount of data involved and the uncertainty of the target location. One possibility is to use reference surfaces, obtained by independent optical methods (e.g. terrestrial laser, photogrammetry). Nevertheless, such an approach is very costly and time consuming, despite the fact that the resulting accuracy may be comparable or even inferior to that obtained by high resolution airborne laser scanning. Hence the easiest and most cost-effective way for assessing data quality remains in the use of data overlaps, although it determines only the internal accuracy of the data. This method was applied for evaluating the coherence of our predicted point-cloud accuracy with that obtained by post-processing. As a base for comparison we have established two scenarios:

A. Flight with good GPS data ($\sigma_{XYZ} < 0.1$ m), where the ambiguities can be fixed with high confidence level.

Please cite this article in press as: Skaloud, J., et al., Real-time registration of airborne laser data with sub-decimeter accuracy. ISPRS Journal of Photogrammetry and Remote Sensing (2010), doi:10.1016/j.isprsjprs.2009.12.003

Table 1
Summary of the ALS position estimates for the RTK-radio/fixed-base flight in two flight lines. The solution statistics are calculated for the integral part of the flight. The last line of the table (on flight line) refers to the percentage of time when laser scanning is active.

Solution type	Epochs (%)	Mean differences (m)			Standard deviation (m)			RMS (m)
		X	*Y*	*Z*	*X*	*Y*	*Z*	*XYZ*
Standalone	15.7	0.01	0.03	−0.10	0.06	0.11	0.17	0.23
Float	0.0	–	–	–	–	–	–	–
Fixed	84.3	0.01	0.02	−0.08	0.03	0.05	0.08	0.13
On flight line	41.7	0.02	0.03	−0.07	0.03	0.07	0.10	0.15

Table 2
Summary of the ALS position estimates for the RTK-GPRS/VRS flight in four flight lines. The solution statistics are calculated for the integral part of the flight. The last line of the table (on flight line) refers to the percentage of time spent when laser scanning is active.

Solution type	Epochs (%)	Mean differences (m)			Standard deviation (m)			RMS (m)
		X	*Y*	*Z*	*X*	*Y*	*Z*	*XYZ*
Standalone	5.2	0.08	0.07	0.17	0.53	0.22	0.16	0.62
Float	4.8	0.58	0.08	0.08	0.33	0.25	0.29	0.78
Fixed	90.1	−0.01	−0.01	0.06	0.08	0.05	0.06	0.13
On flight line	71.5	0.03	−0.01	0.02	0.11	0.08	0.08	0.16

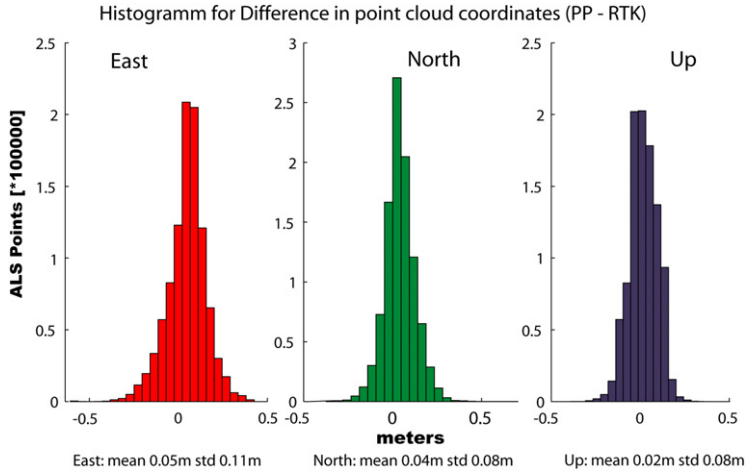

Fig. 7. Histograms of difference in point-cloud coordinates computed in real-time and in post-processing for the second flight (RTK by GPRS, based on down-sampled data).

Table 3
A priori accuracies for ALS system and test data flight parameters.

System calibration parameters/incertitude	
Boresight	$\sigma_r = \sigma_p = 0.002$ deg $\sigma_y = 0.007$ deg
Leverarm	$\sigma_{ax} = \sigma_{ay} = \sigma_{az} = 0.01$ m
Intrinsic ALS parameters/incertitude	
Range-finder	$\sigma_\rho = 0.02 + 20$ ppm
Encoder angle	$\sigma_\theta = 0.005$ deg
Beam width	$\gamma = 3$ mrad
Flight parameters	
Mean point density	$d \approx 6$ points/m^2
Av. height over ground	$h = 250$ m

B. Flight with critical GPS data; the resolution of the ambiguities in post-processing is partially impossible.

The data set for scenario B was generated by artificially degrading the GPS data set used in scenario A (i.e. removing the signal of several satellites). The original data set was acquired using the previously described Scan2map system. The system uncertainties and flight characteristics are summarized in Table 3.

5.2. Positioning and point cloud prediction

Fig. 8 depicts the general layout of this evaluation. The continuous line indicates the smoothed navigation RMS error in height of the "original" data (scenario A), whereas the dashed line represents the height RMS of the data used for scenario B. Fig. 8 shows that the first strip (strip 1) has similar navigation and thus point-cloud accuracy in both scenarios (used as a reference strip), whereas the second strip (strip 2) is affected by important degradation of the GPS positioning quality in scenario B. This is further highlighted in Fig. 9, where for scenario A, the GPS quality flags remain good (green colored) throughout strip 2, whereas in scenario B the predicted GPS positioning quality oscillates between critical and bad (orange and red colored). The difference can also be seen in the *q*-indicator map in the same figure, where for scenario B ($\bar{q}_i = 0.40$ m) the average quality indicator is 8 cm larger than for scenario A ($\bar{q}_i = 0.32$ m). Additionally, the quality maps reflect very well the spatial non-homogeneity in the point-cloud accuracy. For instance, it is evident that the points scanned at the outer borders of the swath have reduced accuracy. This fact is explainable by the less favorable incidence angle as compared to points acquired in the middle of the strip, where the laser shot is almost perpendicular to the terrain.

5.3. Validation

To assess the correctness of the predicted quality maps, we have computed height difference grids between the overlapping parts of strip 1 (used as a reference strip) and strip 2 for both scenarios (Fig. 10). Additionally, we computed 3-dimensional strip differences using the ICP (Iterative Closest Point search) algorithm

Please cite this article in press as: Skaloud, J., et al., Real-time registration of airborne laser data with sub-decimeter accuracy. ISPRS Journal of Photogrammetry and Remote Sensing (2010), doi:10.1016/j.isprsjprs.2009.12.003

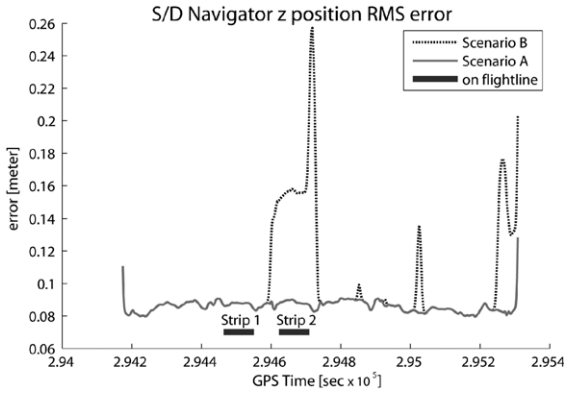

Fig. 8. Comparison of the smoothed navigation RMS error in height for both scenarios.

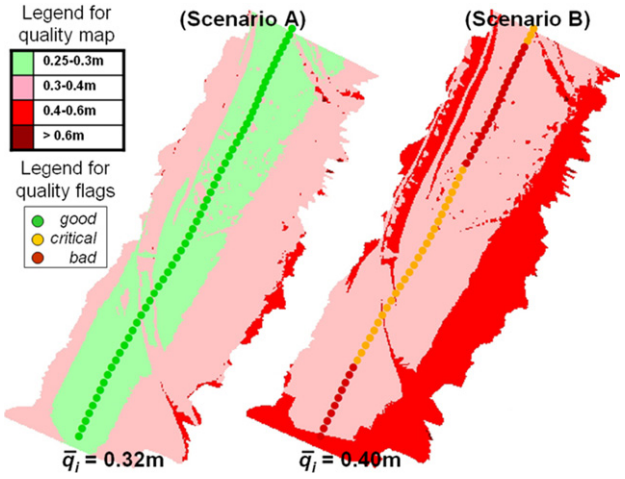

Fig. 9. GPS quality flags (dots) and q-indicator quality maps computed in-flight for strip 2 for both scenarios.

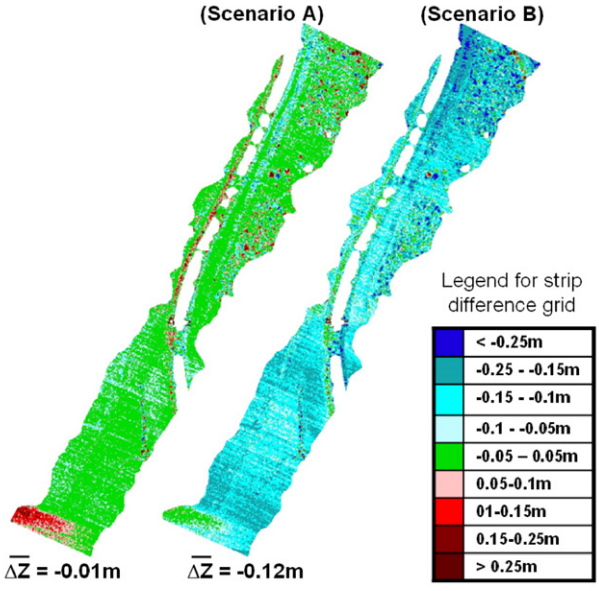

Fig. 10. Height difference grids (strip 2 minus strip 1) computed for the overlapping parts of strip 1 and 2 for both scenarios.

for data matching and strip adjustment. This approach provided global 3D translation parameters between the two adjacent strips. Table 4 summarizes the obtained discrepancies with ΔXYZ

Table 4
Comparison of the 3D strip differences (strip 2 minus strip 1) computed by ICP with the mean real-time quality indicator for strip 2.

Scenario	Strip differences on post-processed point cloud					Real-time quality map
	ICP				Grid	$\bar{q}_i$ (m)
	ΔX (m)	ΔY (m)	ΔZ (m)	$\lvert\Delta XYZ\rvert$ (m)	$\overline{\Delta Z}$ (m)	
A	0.08	0.05	−0.01	0.09	−0.01	0.32
B	0.12	0.18	−0.11	0.24	−0.12	0.40

differences computed by ICP and the mean $\overline{\Delta Z}$ computed by the height difference grids. These values can be compared with the mean quality indicators ($\bar{q}_i$) as predicted during the flight. Values for the norm ($|\Delta XYZ|$) of the 3D displacement computed by ICP and the mean quality indicator do not correspond completely, but the order of magnitude is similar. The difference is explainable by the contribution of the laser footprint size to the computation of q_i: for an average height above the terrain of 250 m and a beam divergence of 3 mrad, the resulting footprint on the ground is larger than 0.6 m, thus contributing largely to the q_i-value. This reduced spatial resolution due to beam focus is partially recovered by the high spatial sampling (6 points/m^2). We can also say that there is a difference of concept: the q_i-indicator map represents the accuracy for every laser point individually, whereas the ICP recovers the differences of two data sets considering all laser points together as one single model. Obviously, if the mean point density is high, mapping the q_i-indicator provides a rather too pessimistic estimation of 3D accuracy of the obtained height model. On the other hand, if we focus on the recovery of fine geometrical structures (e.g. break-lines, corners, targets), the presented quality map is realistic.

6. Summary

In this paper we have first described a methodology for real-time generation of the laser point cloud from moving platforms and time-delayed monitoring of the obtained accuracy. Secondly, we have identified and tested two communication technologies suitable for airborne RTK positioning. We have also described an approach for a positioning quality prediction that is suited for cases when transmission of the phase-corrections is not established. Thirdly, we have compared the real-time generated point cloud to that obtained by post-processing. From that comparison we have concluded that whenever a RTK-fixed solution is obtained, and that was 90% of the cases, the respective differences in the laser point-cloud coordinates are not significant for a majority of ALS applications (i.e. smaller than 0.1 m). Finally, we have validated the positioning component for the purpose of in-flight ALS quality monitoring. This added to the remaining link to our previous efforts in achieving complete monitoring of ALS quality parameters in flight in terms of homogeneity, completeness and accuracy. Although our experience is limited to one system, it serves as a proof of concept for a new approach to ALS data collection, the benefits of which are multiple:

- As the whole chain of "basic data processing" gets automated, the method of airborne laser scanning becomes more economical and faster in production.
- The quality of all data sources can be checked comprehensively and directly within the flight. This issue is particularly crucial for the satellite phase observations.
- The technology is feasible for a new type of monitoring missions requiring short reaction time.

Please cite this article in press as: Skaloud, J., et al., Real-time registration of airborne laser data with sub-decimeter accuracy. ISPRS Journal of Photogrammetry and Remote Sensing (2010), doi:10.1016/j.isprsjprs.2009.12.003

Acknowledgements

This project was partly founded by the Swiss Commission for Innovation (CTI/KTI project 7782.1 EPRP) in collaboration with Swissphoto AG. The GIINAV software is licensed to EPFL by the fourth author of the present paper.

References

Bae, K., Lichti, D., 2004. Automated registration of unorganised point clouds from terrestrial laser scanners. International Archives of Photogrammetry, Remote Sensing and Spatial Information Sciences 3 5 (Part B5), 222–227.

Filin, S., Vosselman, G., 2004. Adjustment of airborne laser altimetry strips. International Archives of Photogrammetry, Remote Sensing and Spatial Information Sciences 34 (Part B3), 285–289.

Glennie, C.L., 2007. Rigorous 3D error analysis of kinematic scanning LIDAR systems. Journal of Applied Geodesy 1 (3), 147–157.

Kong, X., Nebot, E.M., Durrant-Whyte, H., 1999. Development of a non-linear psi-angle model for large misalignment errors and its application in INS alignment and calibration. In: IEEE Proceedings of the International Conference on Robotics and Automation Detroit, MI, USA, May 10–15, pp. 1430–1435.

Legat, K., 2006. Approximate direct georeferencing in national coordinates. ISPRS Journal of Photogrammetry and Remote Sensing 60 (4), 239–255.

Ober, P.B., 2001. SBAS integrity concept. Eurocontrol, Brussels, p. 63.

Pfeifer, N., Oude, E., Filin, S., 2005. Automatic tie elements detection for laser scanner strip adjustment. The International Archives of the Photogrammetry, Remote Sensing and Spatial Information Sciences 36 (Part 3/W19), 8 (on CD ROM).

Schaer, P., Skaloud, J., Landtwig, S., Legat, K., 2007. Accuracy estimation for laser point cloud including scanning geometry. The International Archives of the Photogrammetry, Remote Sensing and Spatial Information Sciences 36 (Part 5), 8 (on CD ROM).

Schaer, P., Skaloud, J., Tome, P., 2008. Towards in-flight quality assessment of airborne laser scanning. International Archives of the Photogrammetry, Remote Sensing and Spatial Information Sciences 37 (Part B5), 851–856.

Schenk, T., 2001. Modeling and analyzing systematic errors in airborne laser scanners. Technical Notes in Photogrammetry, vol 19. The Ohio State University, Columbus, USA, p. 46.

Skaloud, J., 2006. Reliability of direct georeferencing phase 1: An overview of the current approaches and possibilities. Checking and Improving of Digital Terrain Models/Reliability of Direct Georeferencing. EuroSDR Official Publication 51, pp. 144–168.

Skaloud, J., Lichti, D., 2006. Rigorous approach to bore-sight self calibration in airborne laser scanning. ISPRS Journal of Photogrammetry and Remote Sensing 61 (1), 47–59.

Tome, P., Cunha, T., Cunha, S., Bastos, L., 2000. Evaluation of a DGPS/IMU integrated navigation system. In: Proceedings of the ION GPS Conference, Salt Lake City, UT, USA, September 19–22, pp. 2233–2242.

Van Diggelen, F., Brown, A., 1994. Mathematical aspects of GPS RAIM. In: IEEE Proceedings of The Position Location and Navigation Symposium. IEEE, Las Vegas, USA, pp. 733–738.

Xu, G., 2007. GPS: Theory, Algorithms and Applications. Springer Verlag, Berlin.

Please cite this article in press as: Skaloud, J., et al., Real-time registration of airborne laser data with sub-decimeter accuracy. ISPRS Journal of Photogrammetry and Remote Sensing (2010), doi:10.1016/j.isprsjprs.2009.12.003